Journal of Materials Chemistry A

Uncovering the Mechanism Governing Initiating the Nucleation of Lead Sulfide Quantum Dots through a Hines Synthesis

Journal:	*Journal of Materials Chemistry A*
Manuscript ID	TA-ART-01-2018-000220.R1
Article Type:	Paper
Date Submitted by the Author:	09-Mar-2018
Complete List of Authors:	Stevenson, James ; Cornell University, School of Chemical and Biomolecular Engineering Ruttinger, Andrew; Cornell University, Chemical and Biomolecular Engineering Clancy, Paulette; Cornell University

Journal Name

ARTICLE TYPE

Cite this: DOI: 10.1039/xxxxxxxxxx

Uncovering the Reaction Mechanism Initiating the Nucleation of Lead Sulfide Quantum Dots in a Hines Synthesis†

James M. Stevenson,[a‡] Andrew W. Ruttinger,*[a‡] and Paulette Clancy[a]

Received Date
Accepted Date

DOI: 10.1039/xxxxxxxxxx

www.rsc.org/journalname

Lead sulfide quantum dots remain the subject of considerable research interest due to their tunable quantum confinement, which leads to exciting photovoltaic and energy storage applications. A major advantage arises from their low-cost fabrication by solution processing. High quality quantum dots can be synthesized in small quantities *via* colloidal synthesis. However, despite remarkable advances in the synthesis of highly monodisperse dots with precisely programmable structure and composition, details of the mechanism involved in the transformation of molecular precursors to nanoscale crystals remains poorly understood. Surprisingly little is known about the early stages of nucleation, including the stoichiometry, structure, or crystallinity of the hypothesized critical nucleus. Notably, these questions are beyond today's experimental capabilities; the best current technique, *in situ* X-ray scattering, still requires theoretical models to invert the experimental data. Using accurate Density Functional Theory (DFT), coupled with the Nudged Elastic Band (NEB) method for energy barrier construction, we have analyzed a previously posited reaction mechanism, uncovered some energetically unfavorable aspects, and discovered a new reaction mechanism with a lower energy pathway to PbS quantum dot formation. This new mechanism validates experimental results by Zherebetskyy *et al.* who revealed the important presence of water molecules in these systems. We provide evidence that the growth of PbS dots occurs in a polymerization-like process, rather than the reactants-to-surface mechanism proposed in earlier work. We also uncover the significant role played by a hydrogen-bonded dimer of lead carboxylate hydrate, which forms in non-polar solvents.

Introduction

Studies of chemical reaction mechanisms and their kinetics have long been one of the pillars of chemistry. While traditionally such studies have been the province of experimentalists through techniques including the pulse method, isotope measurements, and mass spectrometry,[1] these mechanisms are notoriously hard to uncover directly. Invariably, they require a series of creative, but often indirect, experiments to test the details of a proposed mechanism.[2] Single-molecule and -particle fluorescence microscopy appears to be a promising; however, its application to chemistry is still in its infancy.[3] As innovations in chemical syntheses continue to discover new materials, the complexity of the chemical reactions is also impacted. However, understanding the true reaction mechanism could provide the key to engineer the outcome through a more precise control of external reaction conditions or species.[4] This provides considerable motivation to perform a theoretical analysis that can provide missing, or perhaps unanticipated, information. The growth of computational resources in recent years has spurred the development of theoretical tools to undercover reaction mechanisms with atomic-level precision and considerable accuracy.[5,6] More recent advances have even provided the means to automatically determine a reaction coordinate with only knowledge of the reactants and products required.[7] This has promoted the mutual advancement of both theoretical and experimental work through productive collaborations.[8]

One such test case involves the study of lead chalcogenide quantum dots (PbS, PbSe, *etc.*), with exciting opportunities for optical and photovoltaic applications, as well as display technologies. These applications are facilitated by their controllable size distribution, which allows properties to be engineered *via* tunable quantum confinement.[9] However, the properties of quantum dots are very sensitive to their size, making a high monodispersity of

[a] *Robert F. Smith School of Chemical and Biomolecular Engineering, Cornell University, Ithaca NY, USA 14853. Email: awr66@cornell.edu*

† Electronic Supplementary Information (ESI) available: this work includes further description of our use of DFT functionals and basis sets, the method for using the NEB approach for finding the MEP, along with the reasoning for doing so, and Cartesian coordinates of all relevant stationary points and transition states along the reaction coordinate. See DOI: 10.1039/b000000x/

‡ Contributed equally to this work.

quantum dot sizes highly desirable. This has proved non-trivial to maintain as synthesis batches grow larger in scale.[10] So far, the processes that need to be harnessed to create monodispersity are not fully understood, making them difficult to scale up while maintaining structural fidelity.

Despite profound recent advances in high quality PbX quantum dot synthesis, significant knowledge gaps still persist with regards to understanding the fundamental chemical interactions at play prior to the initial nucleation. These knowledge gaps also have important implications on our understanding of the detailed nature of the nanocrystal surface and related electronic (trap) states, which impact the performance of nanocrystal-based optoelectronic devices. Our paper addresses this knowledge gap, namely, uncovering the chemical mechanism that governs the formation of a PbS "monomer" that will initiate nucleation and quantum dot growth using computational methods. We show how this explains not only experimental observations but enriches our understanding and ability to control quantum dot nucleation and growth.

Insight into PbS Quantum Dot Synthesis

A lead sulfide quantum dot is composed of a PbS core which approaches the bulk cubic lattice, with a less-ordered, passivated surface. The currently favored method for synthesizing PbS quantum dots is the Hines synthesis in which lead oleate is the source of lead, and trimethyl silane sulfide (TMS_2S) is the source of sulfur.[11,12] A stoichiometric excess of lead oleate is used in the reaction, causing the surface passivation in this case to be performed by complexes of Pb^{2+} and anionic ligands. As described by Zherebetskyy *et al.*, PbS quantum dot growth will proceed on the passivated surface *via* surface-bound Pb^{2+} and TMS_2S. As the quantum dot grows, its surface area and the amount of passivating Pb^{2+} increases, allowing the reaction to proceed quickly. The sulfur source may be depleted by the reaction, but concentration of the lead compounds and their complexes remains significant throughout. Lead carboxylates have been synthesized for millenia in aqueous solutions (most famously the first artificial sweetener, "sugar of lead"),[13] but understanding their complexation in a non-aqueous solvent is still surprisingly unclear.[14,15] We have discovered evidence that the Hines synthesis involves lead carboxylates in an unexpected form, a dimer, as explained in the Results and Discussion section of this work.

Zherebetskyy *et al.* greatly enhanced our understanding of the role of lead carboxylate in the PbS synthesis with their groundbreaking 2014 paper.[12] This paper uncovered three important facts. First, the lead oleate used in the Hines synthesis is, in fact, a hydrate, with the water molecule so tightly bound to the lead atom that it had not previously been detected. Second, this newly-discovered bound water plays an active role in the PbS nanocrystal synthesis. Third, the resulting nanocrystals now contain hydroxide ligands, in addition to the oleate ligands. As surprising as these revelations may have seemed initially, they resolved several outstanding questions. The oleate ligand is terminated by a rather bulky carboxylate group; the resulting steric hindrance prevents a surface composed of lead ions from bonding with more than one carboxylate group each. However, one carboxylate group (oxidation state -1) is not sufficient to fully passivate a lead ion (oxidation state +2). Further, we know that PbS quantum dots have substantial numbers of excess lead atoms on their surfaces.[16] Zherebetskyy's suggestion that hydroxide ions are present at the quantum dot surface explains all these observations: each lead atom can have two anionic ligands, oleate and hydroxide, without violating steric hindrance, as shown in Figure 1. Thus, excess lead atoms can passivate the whole surface and be passivated themselves at a +2 oxidation state with no contradiction.

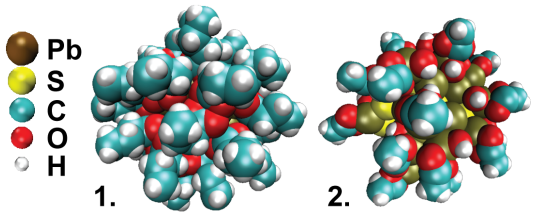

Fig. 1 Density Functional Theory-generated representations of the ligand density surrounding a passivated PbS nanocrystal with (1) no -OH ligands and (2) with -OH ligands as discovered by Zherebetskyy. The state shown on the left exhibits a great deal of steric unfavorability due to overlap between the oxygen atoms. Color key shown to the left of the images.

The mechanism proposed by Zherebetskyy *et al.* is a substitution reaction in which the central sulfur atom of TMS_2S is exchanged with the central oxygen atom of lead oleate hydrate. The two carboxylate groups then join and form $(H_{33}C_{17}\text{-}CO)_2O\text{-}H_2O$. They propose that $(H_{33}C_{17}\text{-}CO)_2O\text{-}H_2O$ later rearranges into a hydrogen-bonded dimer of oleic acid ($H_{33}C_{17}$-COOH), leaving PbS, as described by the equation:

$$(H_{33}C_{17}-COO)_2Pb-H_2O+(CH_3)_3Si-S-Si(CH_3)_3 \qquad (1)$$

$$\rightarrow (CH_3)_3Si-O-Si(CH_3)_3+2(H_{33}C_{17}-COOH)+PbS$$

Zherebetskyy *et al.* tested their mechanism using Density Functional Theory (DFT) studies, but focused solely on the equilibrium states that determine ΔG_{rxn}. In this paper, we shall use transition state DFT, described in the Computational Methods section at the end of the article, and show that the reaction mechanism proposed in Zherebetskyy *et al.*'s paper does not capture the Minimum Energy Pathway (MEP) for the Hines mechanism, particularly during the formation of PbS monomers that precede quantum dot nucleation. The MEP represents the lowest energy reaction coordinate that connects two ground-state energy configurations. This reaction coordinate will encounter an energy barrier and pass through a first-order saddle point (transition state) at its apex. By systematically mapping this MEP to the potential energy surface, we will demonstrate that their proposed mechanism would follow an unfavorable MEP and propose an alternative mechanism, with lower energy intermediates.

Results And Discussion

Understanding the Lead Carboxylate Hydrate

Zherebetskyy *et al.'s* first key insight for the formation of PbS monomers was that lead carboxylate in the Hines synthesis appears in the form of a hydrate.[12] Our calculations fully support this view. The binding energy of the water molecule to the lead carboxylate molecule in toluene is large, 20 kcal/mol, and the resulting Pb-O distance is 2.8 Å, only 0.3 Å greater than the average bond length of the lead carboxylate bonds, 2.5 Å. Therefore, we support their assertion that latent water will remain in lead carboxylate compounds in the hydrate state unless extreme attempts are made to remove it, *e.g.,* by heating or a vacuum.[12]

We find that lead carboxylate hydrate in a non-polar solvent has three isomers which are close in energy, differing in how many internal hydrogen-bonds are formed between the water molecule and the carboxylate ions (Figure 2). Hydrogen bonding is frustrated in a lead carboxylate hydrate molecule because, in order to form hydrogen bonds, the carboxylate ions have to weaken their bonds to the Pb^{2+} ion.

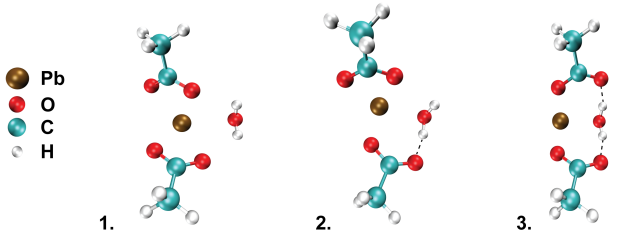

Fig. 2 DFT-derived isomers of the lead carboxylate hydrate. These contain (1) no hydrogen bonds, (2) one hydrogen bond, (3) two hydrogen bonds. Their binding energies (relative to the case without hydrogen-bonding) are (left to right), +0, +0.7, and +3.1 kcal/mol. Despite the general favorability of hydrogen-bonding, the leftmost isomer has the lowest energy because it interferes less with maintenance of Pb-O bonds. Dotted lines represent hydrogen bonds.

As pointed out by Zherebetskyy *et al.*, hydrogen-bonding of the reactants is a strong driver of complexation in nonpolar solvents.[12] However, what was not taken into account is the fact that the same might hold true for the complexation in the lead carboxylate hydrate itself. The frustration of the internal hydrogen bonding in lead carboxylate hydrogen can be resolved if one molecule of lead carboxylate forms a hydrogen-bond with another. This produces the desired hydrogen bonds without other unfavorable changes to the geometry (Figure 3).

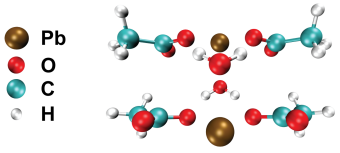

Fig. 3 DFT-derived representation of the structure of a lead acetate hydrate dimer, which we found to be the energetically preferred form of lead acetate in a nonpolar solvent. Note that both hydrogen bonding and the lead-oxygen bonds are fully satisfied in this configuration, with no competition between them.

This result gives lead carboxylate hydrates a strong tendency to dimerize in nonpolar solvents. We found that this dimerization process has no significant energy barrier and a large binding energy of -8.5 kcal/mol/monomer. Dimerization allows all of the hydrogen-bonding of the system to be fully satisfied, while still allowing all the oxygen atoms to bind to the lead. Furthermore, this configuration results in the carboxylate carbon chains pointing in opposite directions, producing no steric hindrance regardless of their lengths. As a result, we believe that the monomer does not play a significant role in the system. Our discovery implies that the dimer form of lead carboxylate hydrate will be the dominant form in nonpolar solvents, including in the Hines synthesis.

We also tested the likelihood of tetramerization, but found it to have a binding energy of only -3.6 kcal/mol/monomer. Considering the entropic contribution of remaining in the dimer state, and the steric hindrance which the tetramer will produce for longer carboxylate carbons chains (Figure 4), this low binding energy makes the lead carboxylate hydrate tetramer unlikely to be a common structure. This is understandable because, having satisfied both lead-oxygen bonding and hydrogen bonding *via* dimerization, there is no obvious driving force for lead carboxylate hydrate to form tetramers, except for electrostatic and van der Waals interactions. Therefore, we can confirm that most lead carboxylate in solution in nonpolar solvent, as in the Hines synthesis for nanocrystals, will be found in the dimerized state.

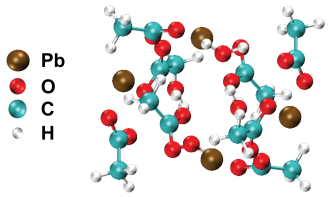

Fig. 4 DFT-generated representation of a lead acetate hydrate tetramer. No more hydrogen-bonding is available, and steric hindrance is beginning to become an issue, making this structure less favorable.

With the monomer-based mechanism proposed by Zherebetskyy *et al.*, the stoichiometry of reactants has a theoretical expectation of 1:1, Pb:S. From their DFT calculations, this ratio was found to be 1.2:1, leaving an excess of lead.[12] However, based on the revelation that the lead is present in the form of a lead oleate dimer, the theoretical stoichiometric ratio of Pb:S would be 2:1 instead. This implies that the 1.2:1 ratio suggested by Zherebetskyy would not leave an excess of lead; instead, lead is the limiting reactant. When Hines synthesized lead sulfide quantum dots, she used a ratio of 2:1 on the basis that the oleic acid concentration would be just enough to provide ligand stability. This ratio was also found to increase lead oleate reactivity.[11] However, we know from Zherebetskyy's work that there exists only one oleic acid per two PbS surface pairs,[12] so -in reality- only a 1:1 ratio is required to satisfy the Hines condition for ligand stability. These seemingly contradictory findings can be elucidated through our discovery of the lead oleate dimer's importance. Rather than having a 2:1 Pb:S ratio for ligand stability, this ratio instead equates to the required 2:1 ratio of lead oleate to sulfur precursor which

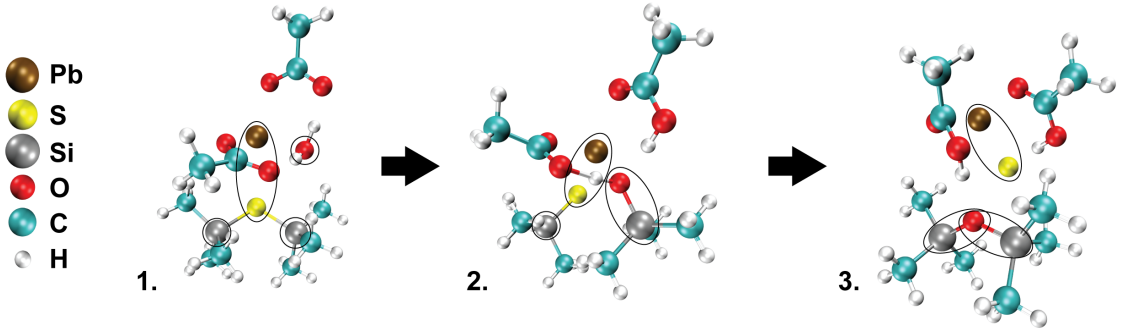

Fig. 5 The Zherebetskyy initialization mechanism proceeding from a bound lead oleate monomer and TMS_2S complex (1). The mechanism passes through an intermediate (2) by the cleavage of a Si-S bond and the formation of a Si-O bond, before forming a PbS quantum dot and its by-products (3) following another Si-S cleavage/S-O formation. Color key for the species is shown on the LHS. The circled species refer to those active in the reaction.

explains Hines' observation of increased reactivity over lower lead oleate concentrations. Moreover, excess oleic acid has been found to improve reactivity. This can be interpreted as faster formation of lead oleate leading to faster dimerization.[17] Conversely, limiting oleic acid limits the formation of lead oleate, which can slow and control quantum dot growth. This can be explained by lead oleate being a limiting reactant, inhibiting dimerization.

Binding to TMS_2S

The next step in the reaction is the binding of the lead carboxylate hydrate with the sulfur source, TMS_2S. This binding, driven by a simple electrostatic interaction between Pb and S, precedes any reaction, but is important because it reduces the concentration of free TMS_2S. For a lead carboxylate hydrate monomer, the binding energy is -15.8 kcal/mol, and for the dimer, -23.9 kcal/mol. These large interaction energies shift the expected equilibrium so far toward the bound state that no free TMS_2S can be expected in the solution once the excess of lead carboxylate is added. This shift in equilibrium has implications for the nucleation and growth stages of the reaction.

Growth Reaction Mechanism

Due to the excess of Pb to TMS_2S in the system, and the strong binding of the TMS_2S to the lead oleate hydrate described above, the initiation reaction would be expected to hold and then consume all of the TMS_2S in the system. This implies that the reaction most likely does not proceed at the surface of the dot as suggested in Zherebetskyy *et al.*'s paper.[12] Instead, we believe it is likely to proceed using the small PbS complexes already formed (which could be considered as tiny embryonic PbS dots), since they are the only remaining source of sulfur in the solution. Therefore, the growth of the dots will occur through a solution-based polymerization of PbS quantum dot monomers, rather than the surface reaction mechanism suggested by Zherebetskyy *et al.*[12] Our study of these pathways in the following sections evaluates the energy profile of the PbS monomer synthesis that would precede this polymerization, rather than the less likely surface reaction.

Zherebetskyy *et al.*'s Initiation Mechanism

Zherebetskyy *et al.* proposed the mechanism given in equation 1. This was suggested on the basis that it is energetically more favorable for water to be bound to the lead oleate than for water to remain free in solution.[12] Then, the water molecule naturally plays an active role in the formation of the PbS monomer (Figure 5). Here, synthesis is initiated by the close proximity of the water molecule to the S atom as well as the affinity of the S atom to leave the TMS_2S and bind with the Pb. This process terminates with the formation of a PbS monomer, with TMS_2O and $H_{33}C_{17}$-COOH as by-products.

To properly model this complex system, care must be taken to ensure the transition states we locate through our calculations correspond to *one* chemical transition (*i.e.* bond cleavage, bond formation). Based on this approach, Zherebetskyy *et al.*'s posited reaction mechanism can be naturally divided into three main steps: 1) binding of a lead oleate monomer to TMS_2S; 2) cleavage of a first S-TMS bond and formation of a first O-TMS bond; 3) cleavage of a second S-TMS bond and formation of a second O-TMS bond. Each step was evaluated separately through determination of its corresponding transition state. Even in simple systems, the search for the desired transition state can be arduous without proper methodology. In our study, we used our custom Nudged Elastic Band (NEB) algorithm to systematically uncover reaction coordinates and predict their transition states, based on the work of Jónsson *et al.*[18] As outlined in the subsequent methods section, we first calculated the MEP at the computationally less intensive B97-D3/def2-TZVP level of DFT theory. This reaction profile is presented in Figure 7 for qualitative comparison with our alternative mechanism. Critical points provided by this reaction profile were then recalculated at the PWPB95-D3/def2-TZVP level of DFT theory for proper quantitative comparison of more physically accurate energies (Figure 8). Details and justification for the necessity of this approach are described in the ESI, along with a comparison of the relative energies of the stationary points at both levels of DFT theory. Through this mechanism, we found a heat of reaction, ΔH_{rxn}, for Zherebetskyy *et al.*'s mechanism of -35.9 kcal/mol, which is favorable, and a maximum activation energy E_a of 32.7 kcal/mol. Even though this transformation has a favorable ΔH_{rxn}, it involves the creation

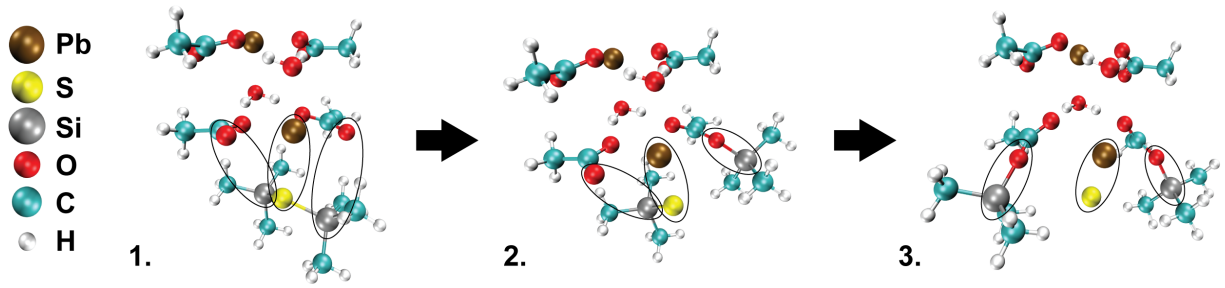

Fig. 6 Our alternative initialization mechanism. The bound lead oleate dimer and TMS_2S (1) react *via* a carboxylate ion and a TMS group to form a stable intermediate (2). Then, the second carboxylate ion and TMS group react to form a PbS species, along with its by-products (3). Color key for the species is shown on the LHS.

of a high-energy intermediate in which the TMS^+ ions, S^{2-} ion, and O^{2-} ion form an unstable cluster. This arises largely from the fact that the sulfur and oxygen atoms must switch places to transform from TMS_2S to TMS_2O, with both TMS^+ ions leaving the sulfur and joining the oxygen.

We also observe that, as the water molecule dissociates in the presence of TMS^+ ions, it strongly prefers to form (TMS)OH rather than TMS_2O. This happens even though the O-H bonds in the water molecule are allowed to, and in fact do, break one at a time during the reaction. The formation of TMS_2O is apparently not likely to occur. A further problem for this reaction mechanism is that it relies on non-dimerized lead carboxylate. As we have shown, lead carboxylate monomers will be rare, making a mechanism which relies on their existence less likely.

The formation of $(H_{33}C_{17}\text{-}CO)_2O\text{-}H_2O$ (oleic anhydride) described in the Zherebetskyy mechanism does not appear to be likely. The formation of oleic acid is not a limiting step in the reaction; it is formed by a simple proton transfer from H_2O to oleic acid, while the formation of oleic anhydride would require further reactions. Furthermore, the acid is more stable than the anhydride+water complex by 13.5 kcal/mol.[19] For these reasons, we believe that the reaction pathway does not include $(H_{33}C_{17}\text{-}CO)_2O\text{-}H_2O$.

To redress these shortcomings, we present an alternative mechanism, which we will demonstrate offers a more kinetically favored route than that originally proposed by Zherebetskyy *et al.*

An Alternative Initiation Mechanism

Our proposed initiation mechanism is given by:

$$[(H_{33}C_{17}-COO)_2Pb-H_2O]_2+(CH_3)_3Si-S-Si(CH_3)_3 \rightarrow \quad (2)$$

$$[PbS][(H_{33}C_{17}-COO)_2Pb-(H_2O)_2]+2(H_{33}C_{17}-COO)-Si(CH_3)_3$$

This hypothesis arises naturally from the geometry of the complex formed by our discovery of the importance of the lead carboxylate dimer and the TMS_2S. In this complex, the carboxylate ions are very close to the silicon atoms of TMS_2S (Figure 6). This suggests that the easiest reaction route is for the TMS_2S silicon to react with a carboxylate oxygen, not with the oxygen atom in the water molecule.

To correctly map the MEP, we again divided up the mechanism, this time into eight steps: 1) cleavage of a first hydrogen bond within the lead oleate hydrate; 2) cleavage of a second hydrogen bond within the lead oleate hydrate; 3) binding of two lead oleate monomers together; 4) dimerization of lead oleate monomers; 5) binding of the lead oleate dimer to TMS_2S; 6) transfer of the first TMS to the first carboxylate ion; 7) rotation of a second TMS towards a second carboxylate ion; 8) transfer of the second TMS to a second carboxylate ion. Using our step-by-step NEB method, we calculated a reaction profile for our proposed mechanism in the same fashion as Zherebetskyy *et al.*'s mechanism: using the B97-D3/def2-TZVP level of DFT theory (Figure 7). We then recalculated the important stationary points with the PWPB95-D3/def2-TZVP level of DFT theory for more accuracy. Again, the relative energies of the mechanism at the B97-D3/def2-TZVP and PWPB95-D3/def2-TZVP levels of DFT theory are compared in the ESI to highlight their quantitative differences.

With the more accurate PWPB95-D3/def2-TZVP level of DFT theory, we found an overall heat of reaction, ΔH_{rxn}, of -35.5 kcal/mol for our mechanism, which is favorable, and an activation energy, E_a, of 32.4 kcal/mol, comparable to that for the Zherebetskyy mechanism (Figure 8). The value of ΔH_{rxn} for this pathway is almost identical to the Zherebetskyy mechanism (-35.9 kcal/mol) and, since DFT was only used to determine the start and end states in Zherebetskyy *et al.*'s paper, their mechanism may appear to be preferable at first glance. However, once the reaction pathways are taken into account (not described in Zherebetskyy's paper), the alternative mechanism we propose here will kinetically dominate the Zherebetskyy mechanism (Figure 7). Neither reaction has a small enough ΔH_{rxn} to be trivially reversed, and the alternative mechanism follows a reaction coordinate through much lower-energy intermediates. Zherebetskyy's mechanism only reaches a minimum relative energy of -35.9 kcal/mol at the completion of the reaction. Our alternative mechanism, however, reaches energies as low as -56.4 kcal/mol, and its stable intermediates remain below -35.9 kcal/mol from the dimerization step until the final product is formed.

Microkinetics of PbS Monomer Formation

Using the MEP and corresponding transition states of both the Zherebetskyy *et al.* pathway and our alternative pathway, we quantified the importance of each pathway through the kinet-

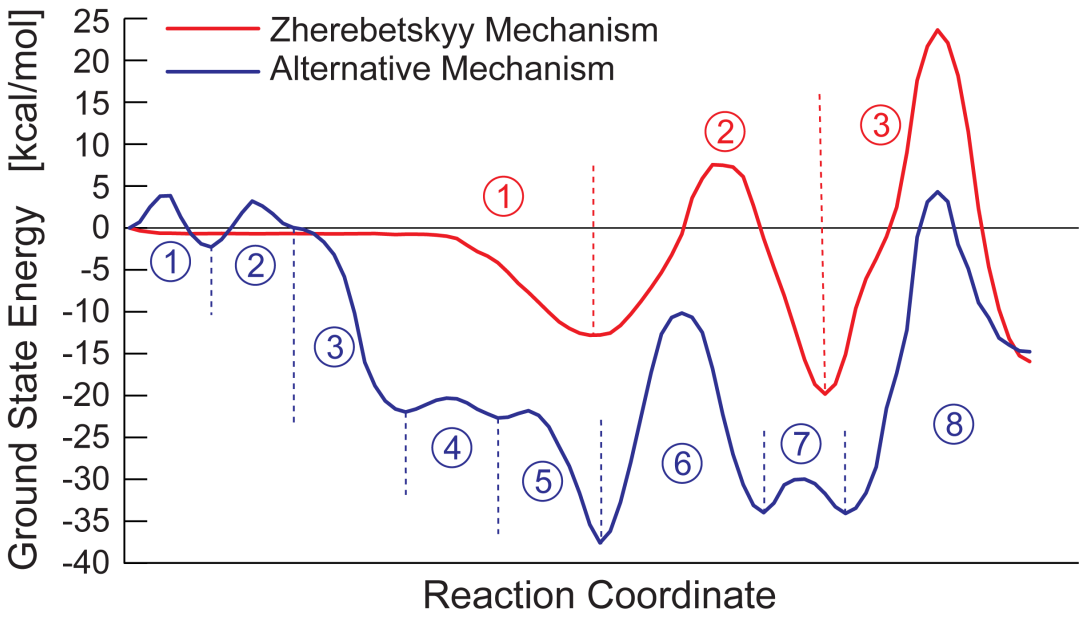

Fig. 7 Comparison of reaction mechanisms between the Zherebetskyy mechanism and the proposed alternative mechanism at the pure DFT level with the B97-D3 functional. Each numbered section corresponds to a single energy barrier and consequently, an individual NEB simulation. The curves represent actual energies along the reaction coordinate.

ics of PbS monomer formation. Knowing the activation energy and vibrational frequencies of each energy barrier, we can apply Transition State Theory (TST) for the barriers of interest.[20] The rate constant for each energy barrier is then given by the Eyring equation:

$$k = \frac{k_b T}{h} \frac{Q^{TS}}{Q^R} e^{-E_a/k_b T} \quad (3)$$

Here, k_b is the Boltzmann constant, T is temperature, h is Planck's constant, and Q is the partition function for either the reactants or the transition state. The partition function we used takes into account individual contributions from translational, rotational, and vibrational partition functions. The electronic partition function was assumed to be unity for both reactant and transition states.

To determine the most kinetically favorable pathway, we looked at likely rate-limiting steps in each pathway. For the Zherebetskyy *et al.* mechanism, this corresponded to barriers 2 and 3; while, for

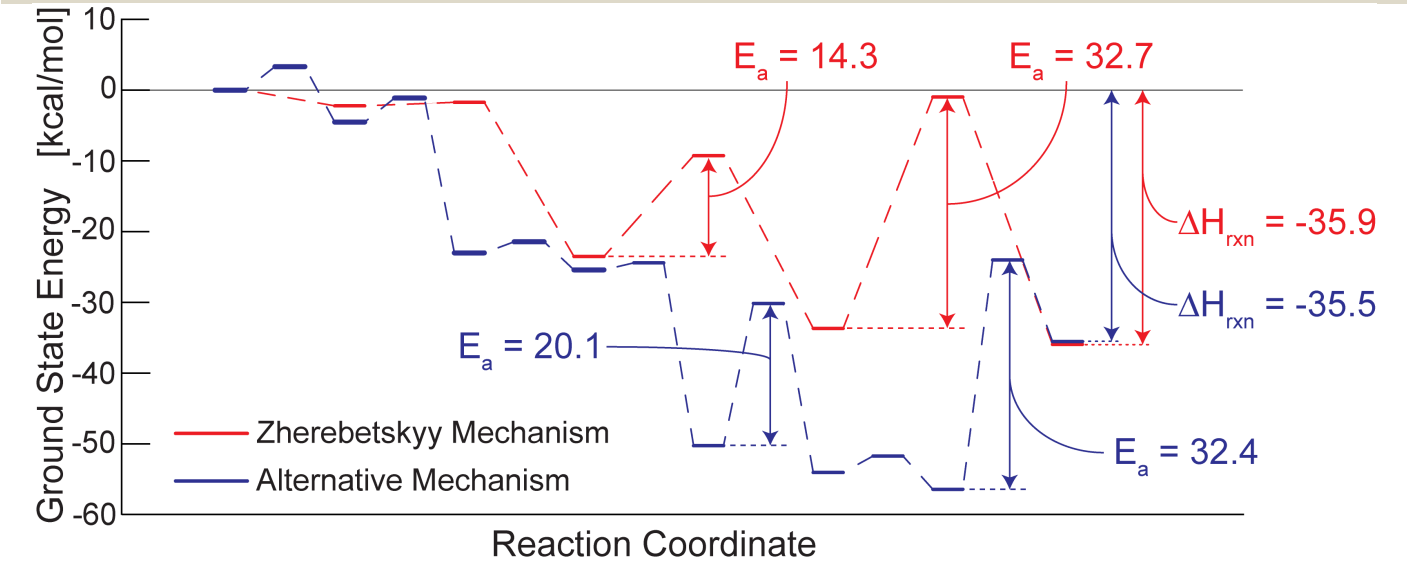

Fig. 8 Comparison of energies between the Zherebetskyy mechanism and the proposed alternative mechanism at the more accurate double hybrid level using a PWPB95-D3 functional. The significant energy barriers for each mechanism (in kcal/mol) are labeled. Only the energies of the minima and transition states were determined at the double hybrid level. Hence the dotted lines are only intended as a guide to the eye, unlike the curves in Fig. 7, where many points were sampled to obtain energies along the entire reaction coordinate.

our alternative mechanism, this corresponded to barriers 6 and 8 (Fig. 7). We do not expect the other barriers to affect the overall kinetics of the reaction due to their relatively small activation energies. All rate constants were calculated at a temperature of 423 K.[11,12] The results are summarized in Table 1.

Table 1 Rate constants for the likely rate-limiting steps in the Zherebetskyy *et al.* mechanism and our alternative mechanism.

Mechanism	Rate constant s^{-1}	Fig. 7 Barrier
Zherebetskyy *et al.*	11300	2
	2.75×10^{-7}	3
Present Work	53.8	6
	1.58×10^{-4}	8

Comparing the rate constants of these rate-limiting steps it is clear that our alternative mechanism dominates the kinetics. This is due to the relative stability of the rate-limiting transition state for our mechanism, compared with the unfavorable complex that forms during the substitution mechanism in the Zherebetskyy *et al.* scheme. Coupled with the low energy intermediates found in our mechanism, these kinetics provide strong justification for the importance of the lead oleate dimer and its subsequent PbS monomer formation.

Conclusions

We have provided new atomic-scale insight into the reasons underlying Zherebetskyy *et al.*'s significant finding that water plays a pivotal role in the formation of PbS quantum dots, which had previously been asserted to be anhydrous. However, the reaction mechanism they suggested is incomplete in two significant ways. First, it assumes that lead carboxylate hydrate in nonpolar solution will exist as a monomer. Second, it involves a high-energy intermediate in the exchange of sulfur for oxygen in $(TMS)_2S$ becoming $(TMS)_2O$, with an activation energy of 32.7 kcal/mol. We have shown that the dominant form of lead carboxylate hydrate in nonpolar solvents is actually a hydrogen-bonded dimer. The tetramer form is not favored over the dimer because it does not produce any new hydrogen bonds. Addressing the second issue, we provide an alternative pathway in which $(TMS)_2O$ forms the carboxylate 2(TMS)COO with an energy barrier of 32.4 kcal/mol, but through much lower energy intermediates. The kinetics of the rate-limiting step for each mechanism support our proposed mechanism, with TST providing a rate constant of $1.58 \times 10^{-4} s^{-1}$ compared to $2.75 \times 10^{-7} s^{-1}$ for Zherebetskyy's mechanism. Using our new customized NEB method, we provide an atomically detailed energy landscape that was previously unknown.

We find that the lead oleate dimer binds to TMS_2S with a binding energy of -23.9 kcal/mol and no significant barrier. As a result of this facile binding, and the fact that lead oleate is added in excess, the amount of unbound TMS_2S will rapidly drop to zero. This rapid depletion of TMS_2S implies that the growth mechanism proposed by Zherebetskyy *et al.*, based on TMS_2S reacting with the surface of a quantum dot, will not be a significant contributor to dot growth. By the time a quantum dot has grown to a substantial size, TMS_2S concentrations will be low. Instead, the quantum dot growth must proceed *via* smaller dots joining with larger ones in an polymerization-like process. These small nuclei, rather than the TMS_2S, should be considered to be the "monomers" of the reaction. The need for small dots to participate can be expected to slow and stabilize dot growth, since the passivating surface groups of the reacting dots must move out of the way before the monomers can bond. Thus, our assertion of a solution-based polymerization mechanism helps to explain why dots from the Hines synthesis achieve their impressive monodispersity.

This new overall reaction mechanism provides information that will help us achieve thermodynamic control over the reactions that lead to the synthesis of PbS and other chalcogenide quantum dots. It should also aid the scale-up of quantum dot synthesis to an industrial scale in which the fidelity of the structure is maintained with molecular-scale precision.

Computational Methods

DFT Calculations

Metal complexes, like the ones at the heart of quantum dot synthesis, present particular challenges for theoreticians to model. First, metal reactions typically require a high level of *ab initio* theory, with large basis sets for isolated systems and large energy cut-offs for periodic systems.[21] Second, because of their many accessible electronic and bonding states, metal complexes have a large number of possible structures, which makes them a challenge to optimize geometrically. Nonetheless, the study of metal complexes is tractable using a combination of fast pure-DFT geometry optimization, hybrid or double-hybrid DFT for energy evaluation,[22] and triple- or even quadruple- zeta basis sets with effective core potentials.[23] Our particular implementation of these techniques is described below.

In this study, we employed two types of DFT calculations. The first type is plane-wave DFT, in which the electron wavefunction is represented by a sum of periodic plane wave basis functions. In plane-wave DFT, users select a functional, which provides the approximations necessary to calculate the energy of a given electron state, and a pseudopotential, a representation of the nuclei and core electrons, over which the plane wave basis adds the outer electrons. Following Zherebetskyy *et al.*, we selected Projector Augmented Wave (PAW) pseudopotentials. We used the commonly used PBE functional[24] and performed our plane-wave calculations using the Quantum Espresso[25] DFT package; details of our implementation are given in the ESI. These calculations were used to validate our second approach, which has substantially faster performance for non-periodic systems such as our PbS monomer formation.

The second type of DFT that we used represents the electron wavefunction with localized orbitals, which Stowasser and Hoffman describe as "a natural language for an *aufbau* of the complex reality of the molecules of the inorganic and organic world."[26] We performed these non-periodic DFT studies, which constitute the bulk of our calculations, using the DFT package Orca,[22] with some initial work in Gaussian 09.[27] Orbital-based methods require a functional, as in plane-wave DFT, and a basis set, which specifies how the orbitals are to be represented in Gaussian-curve basis functions. Details for the initial calculations can be found in

the ESI.

For the final calculations in Orca, we used the fast B97-D3 functional for geometry optimizations, and the double-hybrid PWPB95-D3 functional for the final single-point energy calculations, both recommended in Grimme's DFT benchmark study.[23] We used the RIJK approximation for all integrals.[22] We performed all calculations in Orca with Ahlrichs' def2-*VP family of basis sets,[28–30] which is more accurate than the cc-pV*Z family we used for the initial calculations, at the cost of not being designed to calculate the basis set limit for properties by extrapolation.[31,32] Since we did not use such extrapolation, Ahlrichs' basis sets were more efficient for our application than the cc-pV*Z basis sets. We used the Stuttgart Effective Core Potential (ECP) for lead atoms,[33] as in our initial Gaussian 09 calculations.[34] We represented the solvent using the "COnductor-like Screening MOdel" (COSMO).[35] All of the final energies presented in this work were calculated at the following level of DFT theory: PWPB95-D3/def2-TZVP in COSMO toluene solvent.

To reduce the computational resource demands of the system, we removed the carbon "tails" of the oleate ions after the first C-C single bond, turning them into ethanoates. Past the non-conductive C-C single bond, we have found that the electronic states of the reactive site are essentially unaffected by the presence of the remaining carbon chain, so it can be safely truncated for most purposes.[36] The long carbon chain is necessary in experimental syntheses to improve the solubility, but this is not an issue in our DFT calculations.

Minimum Energy Pathway Determination

In order to determine the activation energy, E_a, of each step of the reaction, we must find all the transition states that are involved. Our chosen method is the popular Nudged Elastic Band (NEB) method for generating reaction pathways.[18] In this method, multiple geometry optimizations between the reactants and products are performed in parallel, each optimization being coupled to the adjacent ones by harmonic constraints which keep the structures geometrically linked. Because neither Orca nor Gaussian 09 support NEB natively, we created a custom NEB driver for both programs.[37] For our justification for selecting the NEB method, as well as an in-depth description of our implementation of the NEB method to find the MEP, refer to the ESI.

To apply the NEB method correctly, the complex PbS monomer formation mechanism was broken down into simple steps, corresponding to the translation of *one* degree of freedom per energy barrier. Then, each energy barrier was studied separately. This careful approach ensured that no energy barriers were being overpredicted. After the transition state of each barrier was located and optimized, the validity of the transition states generated *via* NEB were confirmed through a meticulous approach. The first-order saddle point was confirmed through the existence of one imaginary vibrational frequency, corresponding to an unconstrained degree of freedom. Next, we performed geometry optimizations from either side of each peak and confirmed that these led back to the expected start and end points.[18] The *orca_pltvib* command provides these initial geometries on either side of the peak by visualizing the vibrational mode at the saddle point. Once confirmed, final single point energies were used to predict binding energies, heats of reaction, and activation energies. To prepare our final reaction coordinates, we used an NEB curve-smoothing algorithm described in a recent publication by Kolsbjerg *et al.*.[38]

Conflicts of Interest

The authors declare no competing financial interest.

Acknowledgements

The authors gratefully acknowledge the financial support of NSF GK12 award number DGE-1045513 to Cornell's "Grass Roots: Advancing education in renewable energy and cleaner fuels through collaborative graduate fellow/teacher/grade-school student interactions." The Cornell Institute for Computational Science and Engineering (ICSE) is thanked for the provision of computational resources.

References

1 J. Ross, I. Schreiber and M. O. Vlad, *M. O. Vlad*, Oxford University Press, 2005, pp. 1–6.
2 J. Ross, *Annu. Rev. Mater. Res.*, 2008, **77**, 479âĂŞ494.
3 T. Cordes and S. A. Blum, *Nat. Chem.*, 2013, **5**, 993–999.
4 Y. Zhou and X. Zhuang, *J. Phys. Chem. B.*, 2007, **111**, 13600âĂŞ13610.
5 S. J. Klippenstein, V. S. Pande and D. G. Truhlar, *J. Am. Chem. Soc.*, 2014, **126**, 528–546.
6 G. Henkelman, *Annu. Rev. Mater. Res.*, 2017, **47**, 199âĂŞ216.
7 L. D. Jacobson, A. D. Bochevarov, M. A. Watson, T. F. Hughes, D. Rinaldo, S. Ehrlich, T. B. Steinbrecher, S. Vaitheeswaran, D. M. Philipp, M. D. Halls and R. A. Friesner, *J. Chem. Theory Comput.*, 2017, **13**, 5780–5797.
8 G. Cheng, X. Zhang, L. W. Chung, L. Xu and Y. Wu, *J. Am. Chem. Soc.*, 2015, **137**, 1706âĹŠ1725.
9 I. J. Kramer and E. H. Sargent, *ACS Nano*, 2011, **5**, 8506–8514.
10 R. Debnath, O. Bakr and E. H. Sargent, *Energy Environ. Sci.*, 2011, **4**, 4870–4881.
11 M. A. Hines and G. D. Scholes, *Adv. Mater.*, 2003, **15**, 1844–1849.
12 D. Zherebetskyy, M. Scheele, Y. Zhang, N. Bronstein, C. Thompson, D. Britt, M. Salmeron, P. Alivisatos and L.-W. Wang, *Science*, 2014, **344**, 1380–1384.
13 J. Eisinger, *Med. Hist.*, 1982, **26**, 279–302.
14 P. G. Harrison and A. T. Steel, *J. Organomet. Chem.*, 1982, **239**, 105 – 113.
15 E. E. Bolton, Y. Wang, P. A. Thiessen and S. H. Bryant, *Annu. Rep. Comput. Chem.*, 2008, **4**, year.
16 C. R. Bealing, W. J. Baumgardner, J. J. Choi, T. Hanrath and R. G. Hennig, *ACS Nano*, 2012, **6**, 2118–2127.
17 A. Shrestha, N. Spooner, S. Qiao and S. Dai, *Phys. Chem. Chem. Phys.*, 2016, **18**, 14055–14062.
18 H. Jónsson, G. Mills and K. W. Jacobson, *Nudged Elastic*

Band Method for Finding Minimum Energy Paths of Transitions, World Scientific, 1998, pp. 385–404.

19 F. Becker and A. Maelicke, *Z. Phys. Chem.*, 1967, **55**, 280–295.

20 H. Eyring, *J. Chem. Phys.*, **3**, year.

21 S. Niu and M. B. Hall, *Chem. Rev.*, 2000, **100**, 353–406.

22 F. Neese, *Wiley Interdiscip. Rev. Comput. Mol. Sci.*, 2012, **2**, 73–78.

23 L. Goerigk and S. Grimme, *Phys. Chem. Chem. Phys.*, 2011, **13**, 6670–6688.

24 J. P. Perdew, K. Burke and M. Ernzerhof, *Phys. Rev. Lett.*, 1996, **77**, 3865.

25 P. Giannozzi, S. Baroni, N. Bonini, M. Calandra, R. Car, C. Cavazzoni, D. Ceresoli, G. L. Chiarotti, M. Cococcioni, I. Dabo, A. Dal Corso, S. de Gironcoli, S. Fabris, G. Fratesi, R. Gebauer, U. Gerstmann, C. Gougoussis, A. Kokalj, M. Lazzeri, L. Martin-Samos, N. Marzari, F. Mauri, R. Mazzarello, S. Paolini, A. Pasquarello, L. Paulatto, C. Sbraccia, S. Scandolo, G. Sclauzero, A. P. Seitsonen, A. Smogunov, P. Umari and R. M. Wentzcovitch, *Journal of Physics: Condensed Matter*, 2009, **21**, 395502 (19pp).

26 R. Stowasser and R. Hoffmann, *J. Am. Chem. Soc.*, 1999, **121**, 3414–3420.

27 M. J. Frisch, G. W. Trucks, H. B. Schlegel, G. E. Scuseria, M. A. Robb, J. R. Cheeseman, G. Scalmani, V. Barone, B. Mennucci, G. A. Petersson, H. Nakatsuji, M. Caricato, X. Li, H. P. Hratchian, A. F. Izmaylov, J. Bloino, G. Zheng, J. L. Sonnenberg, M. Hada, M. Ehara, K. Toyota, R. Fukuda, J. Hasegawa, M. Ishida, T. Nakajima, Y. Honda, O. Kitao, H. Nakai, T. Vreven, J. A. Montgomery, Jr., J. E. Peralta, F. Ogliaro, M. Bearpark, J. J. Heyd, E. Brothers, K. N. Kudin, V. N. Staroverov, R. Kobayashi, J. Normand, K. Raghavachari, A. Rendell, J. C. Burant, S. S. Iyengar, J. Tomasi, M. Cossi, N. Rega, J. M. Millam, M. Klene, J. E. Knox, J. B. Cross, V. Bakken, C. Adamo, J. Jaramillo, R. Gomperts, R. E. Stratmann, O. Yazyev, A. J. Austin, R. Cammi, C. Pomelli, J. W. Ochterski, R. L. Martin, K. Morokuma, V. G. Zakrzewski, G. A. Voth, P. Salvador, J. J. Dannenberg, S. Dapprich, A. D. Daniels, Ã. Farkas, J. B. Foresman, J. V. Ortiz, J. Cioslowski and D. J. Fox.

28 A. Schäfer, H. Horn and R. Ahlrichs, *J. Chem. Phys.*, 1992, **97**, 2571–2577.

29 F. Weigand, M. Häser, H. Patzelt and R. Ahlrichs, *Chem. Phys. Lett.*, 1998, **294**, 143–152.

30 F. Weigand and R. Ahlrichs, *Phys. Chem. Chem. Phys.*, 2005, **7**, 3297–3305.

31 F. Weigand, *Phys. Chem. Chem. Phys.*, 2006, **8**, 1057–1065.

32 D. E. Woon and T. H. Dunning Jr, *J.Chem. Phys.*, 1993, **98**, 1358–1371.

33 A. Bergner, M. Dolg, W. Küchle, H. Stoll and H. Preuß, *Mol. Phys.*, 1993, **80**, 1431–1441.

34 J.-Z. Ramírez, R. Vargas, J. Garza and B. P. Hay, *J. Chem. Theory Comput.*, 2006, **2**, 1510–1519.

35 A. Klamt and G. Schüürmann, *J. Chem. Soc. Perkin Trans.*, 1993, **2**, 799–805.

36 F. Maseras and K. Morokuma, *J. Comput. Chem.*, 1995, **16**, 1170–1179.

37 H. Herbol, J. Stevenson and P. Clancy, *J. Chem. Theory Comput.*, 2017, **13**, 3250–3259.

38 E. L. Kolsbjerg, M. N. Groves and B. Hammer, *J. Chem. Phys.*, 2016, **145**, 094107.

Uncovering the Mechanism Governing the Nucleation of Lead Sulfide Quantum Dots through a Hines Synthesis: Table of Contents Graphic

James M. Stevenson, Andrew W. Ruttinger, and Paulette Clancy

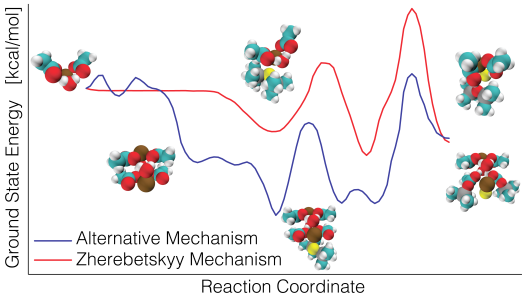

Using computational methods we discover a favorable synthesis pathway towards better control and understanding of quantum dot nucleation for photovoltaics.